



Adsorptive removal of acetaminophen onto acid-modified *Raphia hookeri* fruit epicarp

Adejumoke A. Inyinbor^{1,2} · Deborah T. Bankole^{1,2} · Pamela Solomon¹

Received: 12 October 2022 / Revised: 3 January 2023 / Accepted: 26 January 2023
© The Author(s), under exclusive licence to Springer-Verlag GmbH Germany, part of Springer Nature 2023

Abstract

Cost-effective biochar was prepared from *Raphia hookeri* fruit epicarp following thermal and acid treatment. The potency of the acid-treated biomass (RHP1) was established via physicochemical and spectrophotometric characterization. The acid-treated biomass (RHP1) was subsequently applied for the removal of paracetamol active (PCML). The fixed carbon content of raw *Raphia hookeri* fruit epicarp (63.81%) was enriched after acid treatment. The Brunauer-Emmet-Teller (BET) surface area was also enhanced by acid treatment with 945.43 m²/g obtained for RHP1. The adsorption experimental data subjected to kinetics and isotherm models showed a multilayer adsorption when adsorption data fitted best to the Freundlich isotherm model. The maximum monolayer adsorption capacity (q_{\max}) was 74.04 mg/g. Thermodynamics analysis of the adsorption data showed randomness and endothermic occurrence within the PCML-RHP1 system with ΔH° and ΔS° values of 35.34 kJ/mol and 125.71 J/mol/K respectively. The spontaneity of the adsorption system was validated by the negative values obtained for ΔG° . The mechanism of interaction for RHP1 and PCML was proposed to proceed via hydrogen bonding. RHP1 is therefore a potential tool for the effective treatment of PCML-containing pharmaceutical wastewater.

Keywords *Raphia hookeri* · Paracetamol · Adsorption · Isotherm mode · Kinetic studies

1 Introduction

Environmental contamination is an issue that cannot be ignored, as it can endanger human health and general quality of life. In recent times, a class of pollutants referred to as emerging contaminants has become a concern to environmentalists. These contaminants include insecticides, personal care products, industrial additives, plasticizers, flame retardants, and pharmaceuticals [1]. Besides from preventing and treating diseases, pharmaceuticals and medical therapies have helped to alleviate chronic illness [2]. Some classes of pharmaceuticals are antibiotics, anticonvulsants, sex hormones, mood stabilizers, and analgesic drugs. Paracetamol (PCML) is an analgesic drug that is highly consumed as it is inexpensive with limited side effects [3, 4]. A major concern

arising from the use of PCML is the ability to form a hepatotoxic metabolite (N-acetylimidoquinone). This metabolite can cause DNA damage, coupled with its toxic, mutagenic, and carcinogenic nature [5–7].

The high demand and usage of PCML results in easy detection of the same in the environment in its unmetabolized, metabolized, or expired forms. This can consequently lead to environmental contamination and threat to human health [8]. According to Environmental Health Divisions, United States (2014), paracetamol may inhibit normal reproduction, growth, survival, and embryonic development of fish [9]. Also, the release of wastewater containing pharmaceutical residues can disrupt the aquatic environment by altering the antioxidant mechanism and the metabolism of the biota [3, 7, 8]. It is therefore pertinent to treat wastewater containing this chemical before the discharge into the environment [9, 10]. As reported, several wastewater treatment methodologies have been employed in treating PCML-containing wastewaters. Some of these methods include membrane filtration [11, 12], biological treatments [3, 13], advance oxidation [14, 15], and adsorption [16–18]. These technologies differ in terms of effectiveness, cost and environmental impacts [11, 13]. The adsorption process presents

✉ Adejumoke A. Inyinbor
inyinbor.adejumoke@landmarkuniversity.edu.ng

¹ Department of Physical Sciences, Landmark University, P.M.B 1001, Omu Aran, Nigeria

² Landmark University Clean Water and Sanitation Sustainable Development Goal, Landmark University, P.M.B 1001, Omu Aran, Nigeria

better advantages in terms of cost effectiveness and simplicity of the operation [4, 19, 20].

In recent years, porous activated carbon has been prepared from various waste biomass in order to ameliorate the cost of expensive commercial activated carbon. Agricultural wastes have high carbon content which makes it good substitutes for commercial activated carbons. Some of the agricultural waste previously reported for use as adsorbents include potato peels [21], coconut husk [22], orange peels [18], fenugreek seed spent [23], plantain peels [24], dika nut wastes [25], and *Bilghia sapida* seed pods [26] among others. *Raphia hookeri* is a member of the *Palmicea* family containing high carbon content and high cellulosic fibers, hence present good properties suitable for activated carbon (AC) preparation [27].

Our previous work treated *Raphia hookeri* fruit epicarp with sulphuric acid in a 1:1 mass to volume. Adsorbent obtained had low surface area and was effective for the targeted adsorbate [28]. Commercial activated carbon is characterized with large surface area [29]; hence, we further search for alternative adsorbent that will be a perfect replica in effectiveness and characteristics. The characteristics of activated carbon prepared from agrowastes depends greatly on activating agent, thermal treatment, impregnation ratio, and preparation technique among others [30]. We therefore further explore this neglected waste (*Raphia hookeri*) whose counterpart had found use in commercial activated carbon preparation. In this work, a novel treatment combining H_3PO_4 impregnation with pyrolysis was used to obtain a highly porous material from *Raphia hookeri* biomass. The prepared carbon was for the first time tested for its potential in PCML removal from aqueous solution. Mechanism and feasibility of the adsorption process were established via kinetics and isothermal treatment of data. Surface interaction was used to justify PCML uptake mechanism. The desorption studies as well as the degree of reversibility of the adsorption process were also evaluated.

2 Materials and methods

2.1 Materials

The paracetamol active ingredient with CAS number = 103–90-2; molecular weight = 161.16 g/mol; chemical formula = $C_8H_9NO_2$ and $pK_a = 9.38$ was graciously gifted by May and Baker Pharmaceuticals, Lagos, Nigeria. The reagents that were utilized in this study were all of analytical grade. Deionized water was used throughout the experiment.

2.2 Sample pre-preparation

Raphia hookeri epicarp was obtained from local farmers in Omu-Aran, Kwara State, Nigeria. The acquired raw samples were washed clean with deionized water to ascertain proper removal of

dirt. The samples were then dried at 80 °C for 24 h in the oven. The dried samples were first reduced in size, subsequently pulverized and sieved through 150–215 μm mesh size. The resulting sample was then washed with deionized water till the filtered water was clean, and dried at 80 °C for 48 h in the oven. The samples were properly packed in an air tight container and labeled as RHP.

2.3 Biowaste activation and carbonization

Concentrated orthophosphoric acid with CAS number = 7664–38-2; molecular weight = 97.99 g/mol; percentage purity = 98%; and chemical formula = H_3PO_4 was used in the activation of *Raphia hookeri* epicarp. A total of 20.0 g of the raw adsorbent sample was carefully weighed into a beaker containing 400 ml of the activating reagent. The content was mixed evenly while being heated, till a uniform paste was achieved. The resulting paste/mixture was then moved into an evaporating dish and placed in a furnace for 2 h at 400 °C. This was then cooled down, washed thoroughly using deionized water to a neutral pH, allowed to dry in the oven for 24 h at 100 °C. The product was milled into powder and sieved to a uniform size using a mesh of 106 μm and stored away from moisture with label RHP1.

2.4 Characterization of RHP1

Using a micrometric porosity and surface area analyzer (Micrometric, ASAP 2010 BET), the Brunauer–Emmett–Teller (BET) specific surface area was estimated. For the surface functional group determination, the biochar was degassed in a vacuum for 12 h at 110 °C. The Fourier transformed infrared (FTIR) spectroscopy (NICOLET iS5) was utilized in analyzing the prominent surface functional groups of the prepared biochar. These functional groups are of great importance for the adsorption of PCML onto the surface of RHP1. The surface morphology, characteristic features, and the elemental composition of RHP1 were analyzed utilizing the scanning electron microscopy-electron dispersive X-ray (SEM–EDX) (JEOL JSM-7600F).

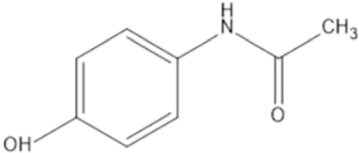
2.5 Paracetamol (PCML) adsorbate preparation

The properties of the paracetamol (PCML) used in this study is presented in Table 1. A total of 200 mg/L of PCML stock solution was prepared by dissolving 0.2 g of PCML active ingredient in 1000 ml of deionized water. The PCML stock solution was further used to make different concentrations of PCML (5, 10, 15, 25, and 50 mg/L), in separate standard flasks.

2.6 PCML-RHP1 batch adsorption studies

The influence of pH on the adsorption of PCML onto RHP1 was first investigated. A total of 0.1 g of the biochar was mixed

Table 1 Properties of paracetamol

Properties	Values
Suggested name	Paracetamol
C.I number	391
C.I name	Acetaminophen
Class	Analgesic drug
λ_{\max}	244
Molecular formula	$C_8H_9NO_2$
Molecular weight	151.163 g/mol
Chemical structure	

with 100 mL solution of 2.5 mg/L initial concentration, within the pH range of 2–11, the mixture was agitated for 4 h. The pH of PCML in solution was varied by the addition of 0.1 M HCl or 0.1 M NaOH. The influence of different amounts (0.15–0.25 g) of RHP1 dosage at initial concentration of 30 mg/L PCML active, which was agitated for about 4 h, was established. Studying the initial concentration, contact time, and temperature effects, 0.1 g of RHP1 was introduced to a predetermined concentration (5–25 mg/L) of the adsorbate solution in a 250 mL conical flask which was agitated at different time interval in a water-bath shaker with varying temperatures (298–318 K). The amount adsorbed at a given time, t , was evaluated using Eq. 1 and removal percentage was calculated using Eq. 2.

$$qt = \frac{(C_i - C_t) \times V}{M} \quad (1)$$

$$\% \text{Removal} = \frac{(C_i - C_f)}{C_i} \times 100 \quad (2)$$

where C_i is the initial concentration, C_t is the concentration of paracetamol at time, and C_f is the final concentration of paracetamol. V is the volume of paracetamol solution used for the adsorption studies in liter and M is the weight of the adsorbent in grams.

2.7 Kinetics and isothermal studies of RHP1-PCML adsorption data

Understanding the modes and mechanisms of adsorbate uptake onto the adsorbent is established by kinetics and equilibrium

adsorption data analysis using a variety of isothermal and kinetics models. Isothermal models include the Langmuir [31], Freundlich [32], Temkin, and Dubinin-Radushkevich (D-R) [33].

Langmuir isotherm assumes a monolayer adsorption onto a uniform surface with a limited number of identical sites. The Langmuir linear form denotes Eq. (3):

$$\frac{C_e}{Q_e} = \frac{1}{K_L Q_{\max}} + \frac{C_e}{Q_{\max}} \quad (3)$$

The exponential distributions of active sites and their energies, as well as surface heterogeneity, are all expressed by the Freundlich sorption isotherm. The Freundlich equation is presented in Eq. (4)

$$\text{Log} q_e = \text{Log} K_F + \frac{1}{n} \log C_e \quad (4)$$

Temkin adsorbent-adsorbate interactions are specifically taken into consideration by Temkin isotherm factors. The model implies that, as a result of this interaction, the heat of adsorption for all molecules in the layer would fall linearly with surface coverage. The linear form is provided in Eq. (5)

$$Q_e = \frac{RT}{b_t} \ln A_T + \frac{RT}{b_t} \ln C_e \quad (5)$$

Dubinin-Radushkevich (DR) explains the adsorption mechanism with a Gaussian energy distribution onto a heterogeneous surface. The results from the intermediate range of concentrations and high solute activity have frequently been well fit by the model. The given linear Eq. (6):

$$\ln Q_e = \ln Q_d - A_{D-R} \epsilon^2 \quad (6)$$

The Polanyi potential (ϵ) and the mean energy of adsorption E are described by Eqs. (7) and (8):

$$\epsilon = RT \ln \left[1 + \frac{1}{C_e} \right] \quad (7)$$

$$E = \left[\frac{1}{\sqrt{2A_{D-R}}} \right] \quad (8)$$

Kinetics data were investigated using the pseudo-first-order [34], pseudo-second-order [35], and intraparticle diffusion [36] kinetic models. Their respective linear equations are represented in Eqs. 9, 10, and 11 respectively.

$$\text{Log} (q_e - q_t) = \log q_e - \frac{K_1 t}{2.303} \quad (9)$$

$$\frac{t}{q_t} = \frac{1}{k_2 q_e^2} + \frac{t}{q_e} \quad (10)$$

$$q_t = k_{id}t^{\frac{1}{2}} + C \quad (11)$$

2.8 Thermodynamics studies of RHP1-PCML adsorption system

The impact of temperature variation on the removal of PCML onto RHP1 was investigated. The embedded parameters clarify the spontaneity, nature of interaction, and the feasibility of the adsorption processes. The Gibb's free energy (ΔG^0), enthalpy (ΔH^0), and entropy (ΔS^0) were calculated using Eqs. 12 and 13.

$$\ln K_o = \frac{\Delta S^o}{R} - \frac{\Delta H^o}{RT} \quad (12)$$

$$\Delta G^o = -RT \ln K_o \quad (13)$$

2.9 Desorption studies of PCML uptake onto RHP1

The reusability and cost effectiveness of an adsorbent can be determined via desorption studies [37, 38]. An already PCML-loaded adsorbent was desorbed using de-ionized water, 0.1 M sodium hydroxide, and 0.1 M hydrochloric acid. A total of 0.2 g of the loaded adsorbent was added to 50 mL of each desorbing agent. The desorption efficiency and the degree of reversibility (desorption index) were determined using Eqs. 14 and 15:

$$q_{des} = C_{des} \frac{V}{W} \quad (14)$$

$$\% \text{ Desorption} = \frac{C_{des}}{C_i} \times 100 \quad (15)$$

$$\% \text{ Desorption efficiency} = \frac{q_{des}}{q_e} \times 100 \quad (16)$$

$$\text{Desorption index} = \frac{\% \text{ total PCML removed after adsorption}}{\% \text{ total PCML remained on the adsorbent after desorption}}$$

3 Results and discussion

3.1 Characterization of RHP1

3.1.1 Physicochemical characterization of RHP1

Thermal application to raw RHP may generate organic components instability hence breaking their linkages [39]. Consequently, both moisture and the volatile matters are liberated while the remnant is the carbon rich biochar. The

results of the physicochemical characterization are presented in Table 2. RHP1 presented a highly porous material with a surface area of 945.43 m²/g which is within the range stated for commercial activated carbon [40]. Previous work which utilized *Raphia hookeri* in adsorbent preparation yielded much lower surface area [28]. The large surface area herein obtained suggests that *Raphia hookeri* with structured treatment may serve as a good precursor for commercial activated carbon production. In addition, the high porosity of RHP1 would enhance its adsorptive properties and increase the chances of RHP1-PCML molecules interaction [37, 38]. Other properties such as the moisture content and pH were found to fall within the acceptable range [41].

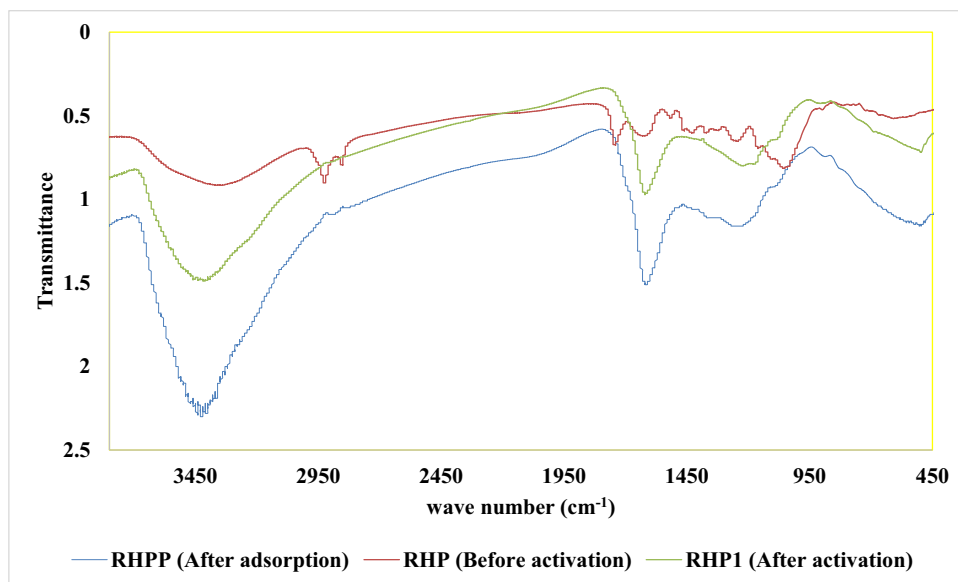
3.1.2 Comparing RHP and RHP1 surface functional group spectral

The surface functional group analyses of RHP and RHP1 are presented in Fig. 1. The effects of PCM uptake on RHP1 have also been compared (Fig. 1). The bands observed at 3400 cm⁻¹ on RHP is a characteristic of -OH stretching vibration. Cellulose, hemicellulose, lignin, and adventitious water in the waste biomass usually facilitate this vibration. The -CH stretching vibration occurring at 2920 cm⁻¹ in RHP disappeared in RHP1. The elimination of volatile organic compounds via thermal and acid treatment may have been responsible for the methylene group disappearance. The band at 1620 cm⁻¹ in RHP is a characteristic of -C=O stretching vibration. The -OH and -C=O group bands also occurred in RHP1 at 3440 and 1610 cm⁻¹ respectively, however, with weak signals. Variations observed in RHP and RHP1 spectral are indication of an effective acid activation [39, 40]. The broadening and band reduction in RHP1 validated the effectiveness of the activation process [42]. Shifts in bands were observed for RHP1 after the uptake of PCML (RHPP), the -OH, and -C=O groups was observed at 3420, 2880, and 1610 cm⁻¹ respectively. The observed changes are indication of the participation of these groups in the

Table 2 Physicochemical properties of RHP1

Property	RHP1
pH	6.10 ± 0.02
pH _{pzc}	4.98 ± 0.02
BET surface area (m ² /g)	945.43
Langmuir surface area (m ² /g)	890.44
Iodine surface area (m ² /g)	772.48
Bulk density (g/cm ³)	0.31
% Moisture content	3.24
% Volatile matter	7.45
% Ash content	10.67
% Fixed carbon	78.64

Fig. 1 FTIR spectra of RHP, RHP1, and RHPP



RHP1-PCML adsorption system. Also weak bands observed in the range of 800 to 500 cm^{-1} are attributed to phosphorus containing compound or aromatic structures [43]. The FTIR spectra of biochar after adsorption (RHPP) showed obvious variation in the carboxylic, hydroxyl, and phosphate groups signify the participation of these functional groups in the RHP1-PCML adsorption process.

3.1.3 Surface morphology and elemental composition spectral of RHP, RHP1, and RHPP

Surface appearances of RHP, RHP1, and RHPP are presented in Fig. 2c–e and a and b are elemental composition of RHP and RHP1. Irregular scanty pores appeared on RHP while thermal and activation generated regular and numerous pores on RHP1 surface. After the uptake of PCML visible blockages of pores was observed, justifying PCML uptake onto RHP1 (Fig. 2c). The elemental analysis depicts carbon content enrichment comparing RHP to RHP1 (Fig. 2a and b). However, oxygen content reduced. The oxygen content reduction further corroborates the elimination of volatile organic compounds as previously shown by the FTIR analysis.

3.2 Effect of pH and adsorption mechanism of PCML uptake onto RHP1

An imperative parameter that significantly influences the efficiency of adsorption is the influence of pH. This study helps to understand the adsorbate-adsorbent interaction. Varying an adsorbate pH can concurrently influence the adsorbent surface charge as well as the adsorbate nature in solution [41, 44]. These changes explain the diverse forms of adsorption mechanism [42–44]. Figure 3 presents graph

of adsorption efficiencies at varying pH. Percentage removal slightly varies as pH increased from 2 to 9 (73.86–78.07%). The highest percentage removal occurred at pH 4. A drastic drop in the removal efficiency was observed from pH 9 to 11 (74.74–40.75%). Paracetamol is a weak electrolyte that can exist in both ionized and non-ionized forms, with a pKa value of 9.38. At $\text{pH} < 9.38$, PCML predominates in its protonated form while its occurrence in solution at $\text{pH} > 9.38$ is predominantly in its deprotonated form. The high removal efficiency observed between pH 2 and 9 can be ascribed to the fact that PCML was adsorbed in its non-ionic form. Hence, electrostatic attraction was not the predominant mechanism of adsorption. The great drop in adsorption efficiency after pH of 9 may, however, be ascribed to electrostatic repulsion between the adsorbent surface and deprotonated PCML. This is because both the PCML molecules and the RHP1 surface are negatively charged. Similar observations have been previously reported [45–47]. Three possible mechanism which include formation of donor–acceptor complexes, hydrogen-bond formation, and π interaction have been proposed for adsorption of contaminants [45]. In the case of RHP1-PCM system, the FTIR before and after adsorption was compared. The intensity of the -OH spectra (3420 cm^{-1}) increased after PCML adsorption and a small peak appeared at 1370 cm^{-1} , indicating the formation of hydrogen bonds. There was a shift in the peak at 1230 cm^{-1} . These changes suggested an interaction between the oxygen group of RHP1 and hydrogen bonded to nitrogen group of the PCML. Hence, hydrogen bonding may be the key mechanism of interaction in the RHP1-PCML system (Fig. 4) [44, 48].

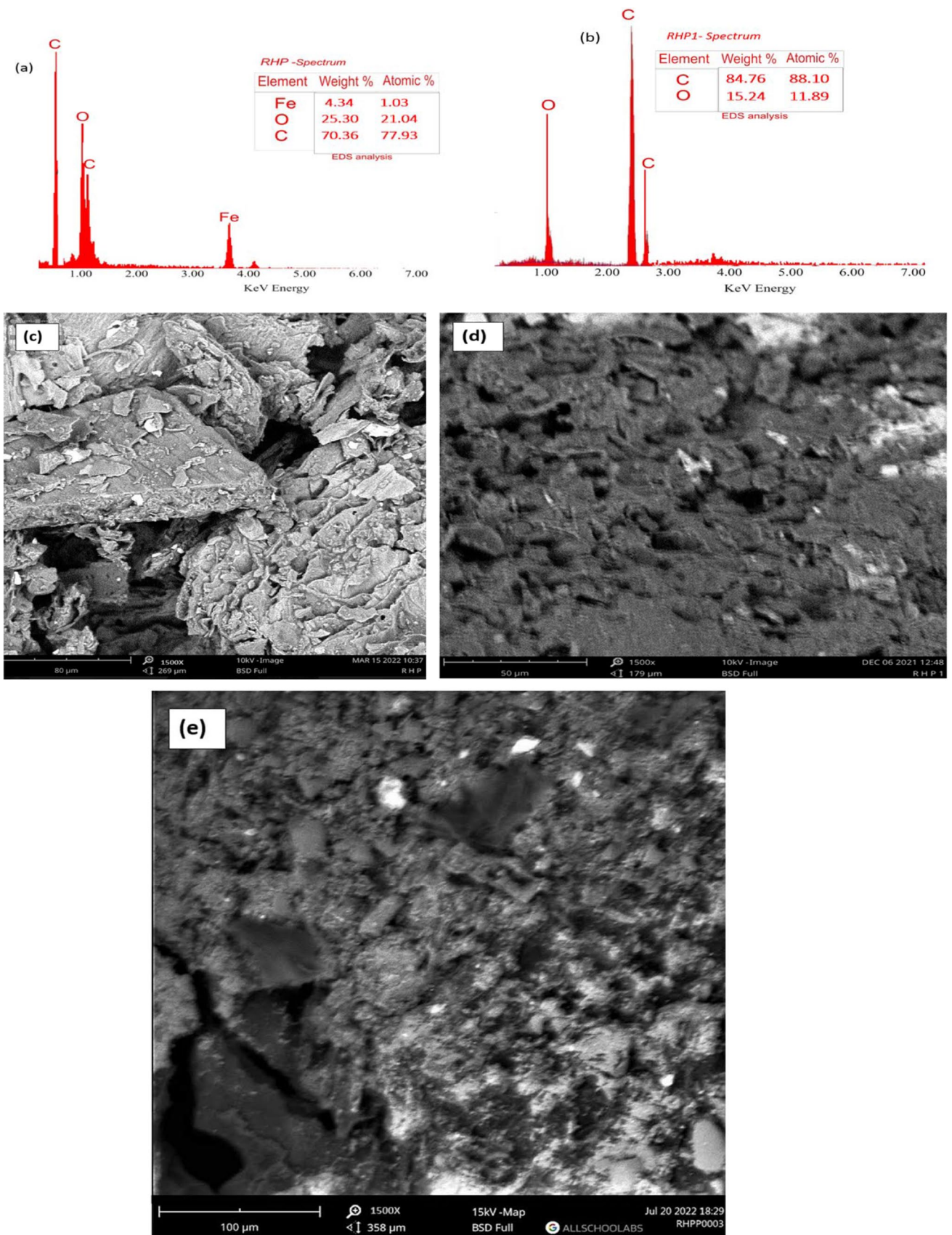


Fig. 2 EDX spectra of **a** RHP and **b** RHP1; SEM morphology of **c** RHP, **d** RHP1, and **e** RHPP

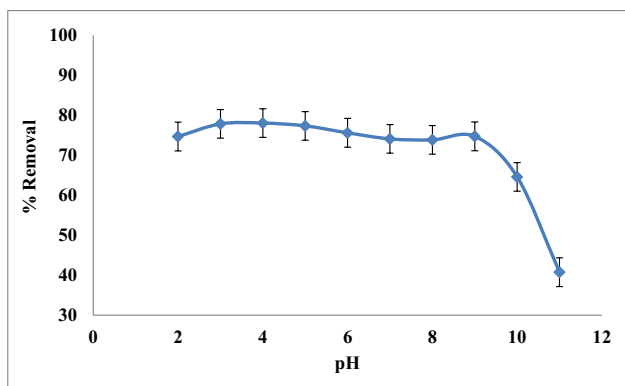


Fig. 3 Effect of pH on PCML adsorption on to RHP1. (Experimental conditions: dosage=0.1 g; initial concentration=25 ppm; volume=0.1 L; contact time=4 h; temperature=298 K, error bars indicating standard deviation of three replicates)

3.3 Effect of initial concentration and contact time on the adsorption of PCML onto RHP1

Figure 5 depicts the adsorbate-adsorbent interactions as a function of time and concentration (5–50 mgL⁻¹) of PCML. The adsorbed quantity of PCML increased rapidly as the initial concentration increased. The quantities adsorbed at equilibrium were 3.43, 10.09, 13.39, 20.29, and 26.77 mg/g for initial concentrations of 5, 10, 15, 25, and 50 ppm. At higher concentrations, there is a high driving force and increased surface bombardment as the time proceeds. As a result, there is an high uptake of PCML onto RHP1 [25]. Adsorption percentage also rises rapidly in the first 30 min and subsequently a gradual removal until removal became insignificant.

3.4 Kinetics studies of PCML uptake onto RHP1

The extent of adsorption process under certain conditions can be analyzed using kinetic models. Hence, the kinetic studies were executed to comprehend the dynamics of PCML-RHP1 adsorption. The pseudo-first order, pseudo-second

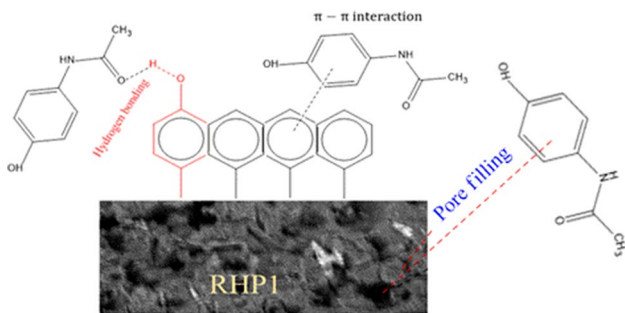


Fig. 4 Possible mechanism of PCML adsorption onto RHP1

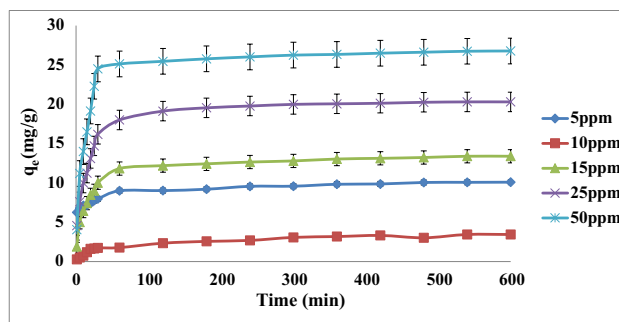


Fig. 5 Effect of contact time and initial concentration on uptake of PCML on to RHP1. (Experimental conditions: dosage=0.1 g; volume=0.1 L; pH=4; temperature=298 K, error bars indicating standard deviation of three replicates; bars fall within symbols where absent)

order, and intraparticle diffusion models were investigated. The calculated parameters from the experimental plots are shown in Table 3. The pseudo-second order model provided the best fit with the R² value of 0.999 for all the concentrations considered. The experimental and the calculated quantity adsorbed (Q_e) for the pseudo second order kinetics were observed to be very close. The intercept (C) of the intraparticle diffusion plot did not pass the through the origin hence an indication of some degree of boundary layer diffusion [49]. Also the values of the intercept of the liquid film diffusion model was not zero, which indicated that the adsorption mechanism is not solely driven by external or surface diffusion [50]. However, the regression coefficients of the intraparticle diffusion across all the concentrations are higher than that of the liquid film diffusion. This is an indication that internal diffusion dominated the adsorption process [51].

3.5 Isothermal studies for PCML uptake onto RHP1

Isotherms are important tool that provides evidence on the capacity of an adsorbent (RHP1) to remove a pollutant (PCML). These models can help to understand adsorbate-adsorbent interactions and their mechanisms. In this work, the Langmuir, Freundlich, Temkin, and Dubinin-Radushkevich isotherms were used to give meaning to the equilibrium adsorption data and the results are presented in Table 4. The maximum monolayer adsorption capacity was enhanced as the temperature increased reaching up to 74.07 mg/g at 318 K. The Langmuir isotherm assumes a monolayer surface, no interactions with neighboring sites, and uniform adsorption energy, whereas the Freundlich isotherm predicted adsorption onto heterogenous sites with varying affinities. The stronger binding sites are initially occupied, and the binding strength decreases with increasing site occupance [52–54]. At room temperature, the Freundlich model provided a better fit

Table 3 Comparison of adsorption kinetic model parameters for PCML uptake onto RHP1

Constants	5 ppm	10 ppm	15 ppm	25 ppm
Pseudo-first order				
Q_e , exp (mg/g)	3.7600	9.850	13.4000	20.3000
Q_e , cal (mg/g)	3.6168	1.6168	2.1256	10.3014
K_1 (min^{-1})	0.01773	0.02579	0.0069	0.0283
R^2	0.9460	0.8680	0.9030	0.9090
Pseudo-second order				
Q_e , cal(mg/g)	3.8100	9.3600	14.0600	21.0600
K_2 (g/mg/min)	3.1326	4.0889	5.0309	7.6240
R^2	0.9990	0.9990	0.9990	0.9990
Intraparticle diffusion				
K_{id}	0.0960	0.2610	0.0110	0.0390
C	0.3023	0.3080	0.3570	0.3040
R^2	0.9990	0.9740	0.9990	0.9980
Liquid film diffusion				
K_{fd}	0.0100	0.0100	0.0100	0.0100
Intercept	0.0879	-0.0102	-0.5647	-0.7282
R^2	0.9208	0.09430	0.9539	0.9601

(0.992) in comparison to the Langmuir model (0.986). This is an indication that a multilayered adsorption predominates the adsorption system. The values of K_L lie between 1 and 10 (1.1456–2.8950), suggesting a favorable adsorption at all temperatures. The high values of B_T for Temkin model indicated a strong interaction between PCML and RHP1 surface. The D-R energy of adsorption was obtained between 50 and 233.61 kJ/mol, which was greater the 8 kJ/mol across all the investigated temperature, indicating a chemical adsorption [55]. The adsorption capacity for paracetamol adsorption was compared to other adsorbents in previous studies (Table 5). The efficacy of RHP1 was justified by high percentage removal compared to previous literature reports.

Table 4 Isothermal studies of the adsorption of PCML onto RHP1

Isotherms	Constants	298 K	308 K	318 K
Langmuir	q_{max} (mg/g)	66.2200	68.9600	74.0700
	R^2	0.9860	0.9730	0.9940
Freundlich	K_f	1.6437	2.895	1.1456
	1/n	0.7330	0.5830	0.7640
	R^2	0.9920	0.9350	0.9850
Temkin	A	1.0050	1.0110	1.0447
	B_T	301.5180	331.9130	213.5580
	b(kJ/mol)	8.2170	7.7150	12.3800
D-R	q_{Dr}	26.7800	23.6300	18.5900
	E	50.0000	129.0900	223.6100
	$\beta \times 10^{-4}$ ($\text{mmol}^2\text{J}^{-2}$)	4.0000	0.6000	0.2000
	R^2	0.8996	0.8114	0.8748

3.6 Effects of temperature and thermodynamic studies of PCML uptake onto RHP1

The quantity of PCML adsorbed increased from 71.37 to 85.99 mg/g as the temperature is raised from 298 to 318 K (Fig. 6). Although, RHP1 is highly effective at ordinary room temperature, increased temperature may have resulted to activation of more adsorption sites on RHP1. The aforementioned coupled with increase in PCML mobility at higher temperatures may account for increased adsorption [56]. The thermodynamic data analysis returned standard enthalpy ΔH° and standard entropy change ΔS° as positive (Table 6). This implies that the adsorption process is random and endothermic in nature. The Gibbs free energy ΔG° values were negative for the temperature range in study, implying the spontaneity and practicability of the adsorption process. Higher negative value obtained at higher temperature further corroborates the higher percentage removal as well as higher maximum monolayer adsorption capacity obtained at higher temperature. This implies that temperature up to 318 K could not break the bonds formed between RHP1 and PCML; hence, RHP1 will be stable while in use in the treatment of hot wastewater.

4 Desorption studies of PCML-RHP1 system

Maximum percentage desorption efficiency of 22.52% was obtained with 0.1 M NaOH (strong acid) eluent (Fig. 7). Desorptions with strong acids and bases have been suggested the participation of ion exchange mechanism [57]. Deionized water eluent performed poorly; thus, the adsorption of PCML onto RHP1 may be through hydrogen bonding and electrostatic attraction. Since the dominant mechanism of interaction is through internal diffusion. The PCML

Table 5 Comparison of various biosorbents for paracetamol adsorption

Adsorbent	Adsorption capacity	Reference
Ozone treated-coconut shells	20.88	[59]
Spent tea leaves	59.20	[60]
<i>Moringa oleifera</i> seed husks	17.48	[61]
Corn cobs	0.47	[62]
Sugarcane bagasse	0.32	[62]
Spiky green horse-chestnut	1.091	[63]
Orange peels	28.09	[18]
<i>Moringa oleifera</i> seed pods	20.28	[64]
Quail egg shells	15.15	[65]
<i>Rahia hookeri</i> epicarp	66.22	This study

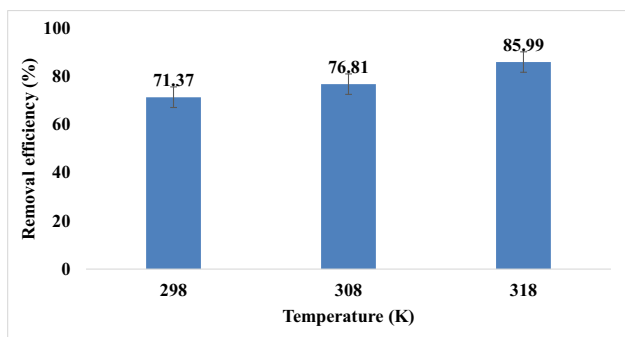


Fig. 6 Effect of temperature on PCML removal on to RHP1. (Experimental conditions: dosage = 0.1 g; initial concentration = 25 ppm; volume = 0.1 L; pH = 4, error bars indicating standard deviation of three replicates)

molecules could penetrate the pores of RHP1, leading to difficult desorption [27]. The values of the desorption index (DI) ranged between 0.91 and 1.19. An adsorption process is completely reversible when the DI equals 1 and as the value deviates from 1, the extent of irreversibility increases [51, 58]. The value of DI for NaOH eluent is 1.19, indicating a slight degree of reversibility.

5 Conclusion

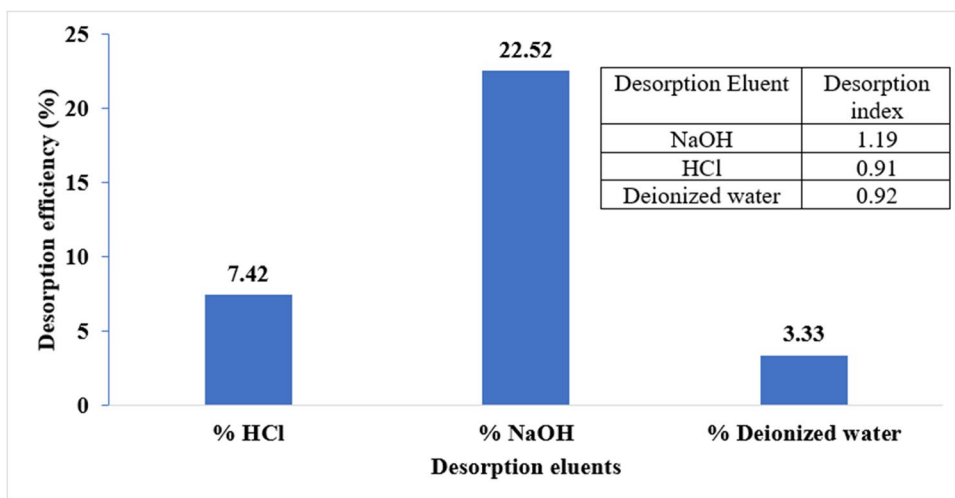
A low-cost biochar (RHP1) was successfully prepared from *Raphia hookeri* waste. The prepared biochar has a large surface area (945.43 m²/g) relative to expectations

for commercial activated carbon, hence, suggests *Raphia hookeri* as a promising precursor for commercial activated carbon preparation. The sorption studies of PCM onto RHP1 revealed that adsorption process is more favorable at pH of 4. Kinetics and equilibrium adsorption data were best described by pseudo-second order kinetic and Freundlich isotherm model. The mechanism of interaction between the PCML molecules and RHP1 surface as deduced from the FTIR spectra was proposed to be via hydrogen bonding. The negative values evaluated from the Gibb’s free energy confirmed the favorability, spontaneity, and the feasibility of the adsorption processes. Feasibility was found to increase with increased temperature and so RHP1 removal efficiency. The intraparticle diffusion predicted that internal diffusion rather than external or surface diffusion dominated the mechanism of interaction between the PCML molecules and RHP1 surface. This may be responsible for the relatively low desorption efficiency (3.33 to 22.52%) obtained for the PCML-RHP1 system. The desorption efficiency, however, indicated slight degree of reversibility of PCML-RHP1 adsorption system with NaOH eluent. The maximum monolayer adsorption capacity (q_{max}) was obtained to be 66.22 mg/g at 298 K and 74.07 mg/g at 318 K, hence, a good PCML removal efficiency even at low temperature systems. The wide availability of *Raphia hookeri* biomass can fortify its future applicability as cost friendly adsorbent for wastewater treatment. The findings of this study would help in keeping sustainable communities, as well as ensure clean water and sanitation.

Table 6 Thermodynamic studies of PCML uptake onto RHP1

Adsorbent	Adsorbate	ΔH° (kJ/mol)	ΔS° (J/mol/K)	ΔG° (kJ/mol)		
				298 K	308 K	318 K
RHP	PCML	35.34	125.71	-2.26	-3.07	-4.79

Fig. 7 Desorption studies of PCML-RHP1 adsorption system



Acknowledgements The authors gratefully acknowledge the provision of facility for research provided by the proprietor of Landmark University.

Author contribution Bankole Deborah: wrote the original draft preparation, wrote reviewing, and edited. Solomon Pamela: data curation, writing original draft, and writing reviewing and editing. Inyinbor Adejumo: conceptualized the idea, wrote the methodology, data curation, writing original draft, and writing reviewing and editing.

Data availability Data used in this work are presented in this paper.

Code availability Not applicable.

Declarations

Ethical approval This work did not involve any clinical trial hence does not require TRN. This work addresses the use of modified agricultural waste as a potential wastewater treatment tool.

Consent to participate Not applicable.

Consent for publication Not applicable.

Competing interests The authors declare no competing interests.

References

- Ramírez-Malule H, Quiñones-Murillo DH, Manotas-Duque D (2020) Emerging contaminants as global environmental hazards A bibliometric analysis. *Emerg Contam* 6:179–193. <https://doi.org/10.1016/j.emcon.2020.05.001>
- Martín-Pozo L, de Alarcón-Gómez B, Rodríguez-Gómez R, García-Córcoles MT, Çipa, Zafra-Gómez A (2018) Analytical methods for the determination of emerging contaminants in sewage sludge samples. A review. *Talanta* 192:508–533, 2019. <https://doi.org/10.1016/j.talanta.2018.09.056>
- Žur J, Wojcieszynska D, Hupert-Kocurek K, Marchlewicz A, Guzik U (2018) Paracetamol – toxicity and microbial utilization. *Pseudomonas moorei* KB4 as a case study for exploring degradation pathway. *Chemosphere* 206:192–202. <https://doi.org/10.1016/j.chemosphere.2018.04.179>
- Lima DR, Hosseini-Bandegharai A, Thue PS, Lima EC, de Albuquerque YRT, dos Reis GS, Umpierrez CS, Dias SLP, Tran HN (2019) Efficient acetaminophen removal from water and hospital effluents treatment by activated carbons derived from Brazil nutshells. *Colloids Surf A Physicochem Eng Asp* 583:123966. <https://doi.org/10.1016/j.colsurfa.2019.123966>
- Pi N, Ng JZ, Kelly BC (2017) Bioaccumulation of pharmaceutically active compounds and endocrine disrupting chemicals in aquatic macrophytes: results of hydroponic experiments with *Echinodorus horemanii* and *Eichhornia crassipes*. *Sci Total Environ* 601–602(1):812–820. <https://doi.org/10.1016/j.scitotenv.2017.05.137>
- Afolabi IC, Popoola SI, Bello OS (2020) Modeling pseudo-second-order kinetics of orange peel-paracetamol adsorption process using artificial neural network. *Chemom Intell Lab Syst* 203:104053. <https://doi.org/10.1016/j.chemolab.2020.104053>
- Kerkhoff CM, Boit MK, Franco DSP, Netto MS, Georgin J, Foletto EL, Piccilli DGA, Silva LFO, Dotto GL (2021) Adsorption of ketoprofen and paracetamol and treatment of a synthetic mixture by novel porous carbon derived from *Butia capitata* endocarp. *J Mol Liq* 339:117184. <https://doi.org/10.1016/j.molliq.2021.117184>
- Agarwal N (2022) Paracetamol - a contaminant of high concern: existence in environment and adverse effect. *Pharm Drug Regul Aff J* 4(1):000128. <https://doi.org/10.23880/pdraj-16000128>
- Environmental Health Division, “Acetaminophen in drinking water,” Clean water, land and legacy amendment. <https://www.health.state.mn.us/eh>. Accessed Aug 2014
- Nunes B (2020) Ecotoxicological effects of the drug paracetamol: a critical review of past ecotoxicity assessments and future perspectives. *Handb Environ Chem* 96:131–145. https://doi.org/10.1007/698_2020_546
- Ahmed MJ (2017) Adsorption of non-steroidal anti-inflammatory drugs from aqueous solution using activated carbons: review. *J Environ Manage* 190:274–282. <https://doi.org/10.1016/j.jenvman.2016.12.073>
- ALothman ZA, Badjah AY, Alduhaish OM, Rathinam K, Panglish S, Ali I (2021) Synthesis, characterization, kinetics and modeling studies of new generation pollutant ketoprofen removal in water using copper nanoparticles. *J Mol Liq* 323:115075. <https://doi.org/10.1016/j.molliq.2020.115075>
- Li J, Zhou Q, Campos LC (2018) The application of GAC sandwich slow sand filtration to remove pharmaceutical and personal care products. *Sci Total Environ* 635:1182–1190. <https://doi.org/10.1016/j.scitotenv.2018.04.198>
- Nadour M, Boukraa F, Benaboura A (2019) Removal of diclofenac, paracetamol and metronidazole using a carbon-polymeric membrane. *J Environ Chem Eng* 7(3):103080. <https://doi.org/10.1016/j.jece.2019.103080>
- Dionisi D, Ettah CC (2019) Effect of process conditions on the aerobic biodegradation of phenol and paracetamol by open mixed microbial cultures. *J Environ Chem Eng* 7(5):103282. <https://doi.org/10.1016/j.jece.2019.103282>
- Yun WC, Lin KYA, Tong WC, Lin YF, Du Y (2019) Enhanced degradation of paracetamol in water using sulfate radical-based advanced oxidation processes catalyzed by 3-dimensional Co₃O₄ nanoflower. *Chem Eng J* 373:1329–1337. <https://doi.org/10.1016/j.cej.2019.05.142>
- Ganiyu SO, Oturan N, Raffy N, Cretin M, Causserand C, Oturan MA (2018) Efficiency of plasma elaborated sub-stoichiometric titanium oxide (Ti₄O₇) ceramic electrode for advanced electrochemical degradation of paracetamol in different electrolyte media. *Sep Purif Technol* 208:142–152. <https://doi.org/10.1016/j.seppur.2018.03.076>
- Afolabi IC, Popoola SI, Bello OS (2020) Machine learning approach for prediction of paracetamol adsorption efficiency on chemically modified orange peel. *Spectrochim Acta - Part A Mol Biomol Spectrosc* 243:118769. <https://doi.org/10.1016/j.saa.2020.118769>
- Leite AB, Saucier C, Lima EC, dos Reis GS, Umpierrez CS, Mello BL, Shirmardi M, Dias SLP, Sampaio CH (2018) Activated carbons from avocado seed: optimisation and application for removal of several emerging organic compounds. *Environ Sci Pollut Res* 25(8):7647–7661. <https://doi.org/10.1007/s11356-017-1105-9>
- Spessato L, Bedin KC, Cazetta AL, Souza IPAF, Duarte VA, Crespo LHS, Silva MC, Pontes RM, Almeida VC (2019) KOH-super activated carbon from biomass waste: insights into the paracetamol adsorption mechanism and thermal regeneration cycles. *J Hazard Mater* 371:499–505. <https://doi.org/10.1016/j.jhazmat.2019.02.102>
- Kyzas GZ, Deliyanni EA (2015) Modified activated carbons from potato peels as green environmental-friendly adsorbents for the treatment of pharmaceutical effluents. *Chem Eng Res Des* 97:135–144. <https://doi.org/10.1016/j.cherd.2014.08.020>

22. Bello OS, Owojuyigbe ES, Babatunde MA, Folaranmi FE (2017) Sustainable conversion of agro-wastes into useful adsorbents. *Appl Water Sci* 7(7):3561–3571. <https://doi.org/10.1007/s13201-016-0494-0>
23. Taqui NS, Mohan CS, Khaton BA, Manzoore EMS, Khan TMY, Mujtaba MA, Waqar A, Elfaskhany A, Ravinder K, Pruncu CI (2021) Sustainable adsorption method for the remediation of malachite green dye using nutraceutical industrial fenugreek seed spent. *Biomass Convers Biorefinery* 0123456789. <https://doi.org/10.1007/s13399-021-01827-w>
24. Nworie FS, Nwabue F, Ikelle II, Ogah AO, Elom N, Illochi NO, Itumoh EJ, Oroke CE (2018) Activated plantain peel biochar as adsorbent for sorption of zinc(II) ions: equilibrium and kinetics studies. *J Turkish Chem Soc Sect A Chem* 5(3):1257–1270
25. Inyinbor AA, Adekola FA, Bello OS, Bankole DT, Oreofe TA, Lukman AF, Olatunji GA (2022) Surface functionalized plant residue in Cu²⁺ scavenging : chemometrics of operational parameters for process economy validation. *S Afr J Chem Eng* 40:144–153. <https://doi.org/10.1016/j.sajce.2022.03.001>
26. Bankole DT, Oluyori AP, Inyinbor AA (2022) Potent adsorbent prepared from Bilghia sapida waste material: surface chemistry and morphological characterization. *Mater Today Proc.* <https://doi.org/10.1016/j.matpr.2022.06.238>
27. Inyinbor AA, Adekola FA, Olatunji GA (2020) Microwave-assisted urea modified crop residue in Cu²⁺ scavenging. *Heliyon* 6(4):03759. <https://doi.org/10.1016/j.heliyon.2020.e03759>
28. Inyinbor AA, Adekola FA, Olatunji GA (2016) Liquid phase adsorption of rhodamine B dye onto acid-treated Raphia hookeri fruit epicarp: isotherms, kinetics and thermodynamics studies. *South African J Chem* 69:218–226. <https://doi.org/10.17159/0379-4350/2016/v69a28>
29. Sinha P, Banerjee S, Kar KK (2020) Characteristics of activated carbon. *Springer Ser Mater Sci* 300:125–154. https://doi.org/10.1007/978-3-030-43009-2_4
30. Njewa JB, Vunain E, Biswick TT (2022) Synthesis and characterization of activated carbons prepared from agro-wastes by chemical activation. *Adsorb Sci Technol* 2022:1–13. <https://doi.org/10.1155/2022/7701128>
31. Langmuir I (1917) The constitution and fundamental properties of solids and liquids. *J Franklin Inst* 183(1):102–105. [https://doi.org/10.1016/S0016-0032\(17\)90938-X](https://doi.org/10.1016/S0016-0032(17)90938-X)
32. Freundlich HM (1906) Over the adsorption in solution. *Z Phys Chem* 57:385–470
33. Dubinin MM, Radushkevich LV (1947) Equation of the characteristic curve of activated charcoal proceedings of the academy of sciences. *Dokl. Akad. Nauk SSSR. Phys Chem Sect USSR* 55:331–333
34. Lagergren S (1898) On the theory of so-called adsorption of dissolved substances. *K Sven Vetenskapsakademiens Handl* 24(4):1–39
35. Ho YS, McKay G (1999) Pseudo-second order model for sorption processes. *Process Biochem* 34(5):451–465. [https://doi.org/10.1016/S0032-9592\(98\)00112-5](https://doi.org/10.1016/S0032-9592(98)00112-5)
36. Weber WJ, Morris JC (1963) Closure to “Kinetics of Adsorption on Carbon from Solution.” *J Sanit Eng Div* 89(6):53–55. <https://doi.org/10.1061/jrsedai.0000467>
37. Khalili H, EbrahimianPirbazari A, Saraei FEK, Mousavi SH (2021) Simultaneous removal of basic dyes from binary systems by modified orange peel and modeling the process by an intelligent tool. *Desalin Water Treat* 221(June):406–427. <https://doi.org/10.5004/dwt.2021.27039>
38. Beltrame KK, Cazetta AL, de Souza PSC, Spessato L, Silva TL, Almeida VC (2018) Adsorption of caffeine on mesoporous activated carbon fibers prepared from pineapple plant leaves. *Ecotoxicol Environ Saf* 147:64–71. <https://doi.org/10.1016/j.ecoenv.2017.08.034>
39. Bello OS, Adegoke KA, Akinyunni OO (2017) Preparation and characterization of a novel adsorbent from Moringa oleifera leaf. *Appl Water Sci* 7(3):1295–1305. <https://doi.org/10.1007/s13201-015-0345-4>
40. Saleem J, Bin Shahid U, Hijab M, Mackey H, McKay G (2019) Production and applications of activated carbons as adsorbents from olive stones. *Biomass Convers Biorefinery* 9(4):775–802. <https://doi.org/10.1007/s13399-019-00473-7>
41. Huang Y, Li S, Chen J, Zhang X, Chen Y (2014) Adsorption of Pb(II) on mesoporous activated carbons fabricated from water hyacinth using H₃PO₄ activation: adsorption capacity, kinetic and isotherm studies. *Appl Surf Sci* 293:160–168. <https://doi.org/10.1016/j.apsusc.2013.12.123>
42. Bello OS, Moshood MA, Ewetumo BA, Afolabi IC (2020) Ibutrofen removal using coconut husk activated biomass. *Chem Data Collect* 29. <https://doi.org/10.1016/j.cdc.2020.100533>
43. Shooto ND (2020) Removal of toxic hexavalent chromium (Cr(VI)) and divalent lead (Pb(II)) ions from aqueous solution by modified rhizomes of Acorus calamus. *Surf Interfaces* 20:100624. <https://doi.org/10.1016/j.surfin.2020.100624>
44. Bello OS, Alagbada TC, Alao OC, Olatunde AM (2020) Sequestering a non-steroidal anti-inflammatory drug using modified orange peels. *Appl Water Sci* 10:172. <https://doi.org/10.1007/s13201-020-01254-8>
45. Baccar R, Sarrà M, Bouzid J, Feki M, Blázquez P (2012) Removal of pharmaceutical compounds by activated carbon prepared from agricultural by-product. *Chem Eng J* 211–212:310–317. <https://doi.org/10.1016/j.cej.2012.09.099>
46. Villaescusa I, Fiol N, Poch J, Bianchi A, Bazzicalupi C (2011) Mechanism of paracetamol removal by vegetable wastes: the contribution of π - π interactions, hydrogen bonding and hydrophobic effect. *Desalination* 270(1–3):35–142. <https://doi.org/10.1016/j.desal.2010.11.037>
47. Nam SW, Choi DJ, Kim S, Her N, Zoh KD (2014) Adsorption characteristics of selected hydrophilic and hydrophobic micropollutants in water using activated carbon. *J Hazard Mater* 270:144–152. <https://doi.org/10.1016/j.jhazmat.2014.01.037>
48. Lladó J, Solé-Sardans M, Lao-Luque C, Fuente E, Ruiz B (2016) Removal of pharmaceutical industry pollutants by coal-based activated carbons. *Process Saf Environ Prot* 104:294–303. <https://doi.org/10.1016/j.psep.2016.09.009>
49. Ojediran JO, Dada AO, Aniyi SO, David RO, Adewumi AD (2021) Mechanism and isotherm modeling of effective adsorption of malachite green as endocrine disruptive dye using Acid Functionalized Maize Cob (AFMC). *Sci Rep* 11(1):1–15. <https://doi.org/10.1038/s41598-021-00993-1>
50. UIHaq A, Shah J, Jan MR, Ud Din S (2015) Kinetic, equilibrium and thermodynamic studies for the sorption of metribuzin from aqueous solution using banana peels, an agro-based biomass. *Toxicol Environ Chem* 97(2):124–134. <https://doi.org/10.1080/0272248.2015.1041528>
51. Dada AO, Adekola FA, Odeunmi EO, Ogunlaja AS, Bello OS (2021) Two–three parameters isotherm modeling, kinetics with statistical validity, desorption and thermodynamic studies of adsorption of Cu(II) ions onto zerovalent iron nanoparticles. *Sci Rep* 11(1):1–15. <https://doi.org/10.1038/s41598-021-95090-8>
52. Nanthamathée C, Chantarangkul C, Jakkrawhad C, Payaka A, Dechatiwongse P (2022) Fine-tuning the dye adsorption capacity of UiO-66 by a mixed-ligand approach. *Heliyon* 8(2). <https://doi.org/10.1016/j.heliyon.2022.e08961>
53. Balarak D, Mostafapour F (2017) Joghtaei A (2017) Thermodynamic analysis for adsorption of amoxicillin onto magnetic carbon nanotubes. *Br J Pharm Res* 16(6):1–11. <https://doi.org/10.9734/bjpr/2017/33212>
54. Abdel-aziz HM, Abdel-gawad SA (2020) Removal of sunset yellow azo dye using activated carbon entrapped in alginate from

- aqueous solutions. *J Sci* 4(1):1–6. <https://doi.org/10.15406/oajs.2020.04.00142>
55. Gorzin F, Bahri Rasht Abadi MM (2018) Adsorption of Cr(VI) from aqueous solution by adsorbent prepared from paper mill sludge: kinetics and thermodynamics studies. *Adsorpt Sci Technol* 36(1–2):149–169. <https://doi.org/10.1177/0263617416686976>
 56. Sun L, Wan S, Yuan D, Yu Z (2019) Adsorption of nitroimidazole antibiotics from aqueous solutions on self-shaping porous biomass carbon foam pellets derived from *Vallisneria natans* waste as a new adsorbent. *Sci Total Environ* 664:24–36. <https://doi.org/10.1016/j.scitotenv.2019.01.412>
 57. Sajab MS, Chia CH, Zakaria S, Sillanpää M (2017) Adsorption of heavy metal ions on surface of functionalized oil palm empty fruit bunch fibres: single and binary systems. *Sains Malaysiana* 46(1):157–165. <https://doi.org/10.17576/jsm-2017-4601-20>
 58. Adekola FA, Hodonou DSS, Adegoke HI (2016) Thermodynamic and kinetic studies of biosorption of iron and manganese from aqueous medium using rice husk ash. *Appl Water Sci* 6(4):319–330. <https://doi.org/10.1007/s13201-014-0227-1>
 59. Yanyan L, Kurniawan TA, Zhu M, Ouyang T, Avtar R, Othman MHD, Mohammad BT, Abadarin AB (2018) Removal of acetaminophen from synthetic wastewater in a fixed-bed column adsorption using low-cost coconut shell waste pretreated with NaOH, HNO₃, ozone, and/or chitosan. *J Environ Manage* 226(April):365–376. <https://doi.org/10.1016/j.jenvman.2018.08.032>
 60. Wong S, Lim Y, Ngadi N, Mat R, Hassan O, Inuwa I, Mohamed NB, Low JH (2018) Removal of acetaminophen by activated carbon synthesized from spent tea leaves: equilibrium, kinetics and thermodynamics studies. *Powder Technol* 338:878–886. <https://doi.org/10.1016/j.powtec.2018.07.075>
 61. Quesada HB, Cusioli LF, Bezerra CO, Baptista ATA, Nishi L, Gomes RG, Bergamasco R (2019) Acetaminophen adsorption using a low-cost adsorbent prepared from modified residues of *Moringa oleifera* Lam. seed husks. *J Chem Technol Biotechnol* 94(10):3147–3157. <https://doi.org/10.1002/jctb.6121>
 62. Juela DM (2020) Comparison of the adsorption capacity of acetaminophen on sugarcane bagasse and corn cob by dynamic simulation. *Sustain Environ Res* 30:23. <https://doi.org/10.1186/s42834-020-00063-7>
 63. Parus A, Gaj M, Karbowska B, Zembruska J (2020) Investigation of acetaminophen adsorption with a biosorbent as a purification method of aqueous solution. *Chem Ecol* 36(7):705–725. <https://doi.org/10.1080/02757540.2020.1757081>
 64. Ogunmodede J, Akanji SB, Bello OS (2021) *Moringa oleifera* seed pod-based adsorbent for the removal of paracetamol from aqueous solution: a novel approach toward diversification. *Environ Prog Sustain Energy* 40(4):1–11. <https://doi.org/10.1002/ep.13615>
 65. Inyinbor AA, Bankole DT, Adekola FA, Bello SO, Oreofe T, Amone K, Lukman FA (2023) Chemometrics validation of adsorption process economy : case study of acetaminophen removal onto quail eggshell adsorbents. *Sci African* 19:e01471. <https://doi.org/10.1016/j.sciaf.2022.e01471>

Publisher's Note Springer Nature remains neutral with regard to jurisdictional claims in published maps and institutional affiliations.

Springer Nature or its licensor (e.g. a society or other partner) holds exclusive rights to this article under a publishing agreement with the author(s) or other rightsholder(s); author self-archiving of the accepted manuscript version of this article is solely governed by the terms of such publishing agreement and applicable law.